DOI: 10.13009/EUCASS2025-154
11TH EUROPEAN CONFERENCE FOR AERONAUTICS AND SPACE SCIENCES (EUCASS)

RD-170 engine start-up transient modelling and analysis

Samuele CORBO[⋆]*, Marco GALEOTTA*[†]*, Marco DE ROSA*[†]*, Francesco NASUTI* [⋆⋆]*, Nicola IERARDO*[†]
[⋆] *ArianeGroup, Vernon, France*
samuele.corbo@me.com
[†]*ESA, European Space Agency*
marco.galeotta@esa.int, marco.de.rosa@esa.int, nicola.ierardo@esa.int
[⋆⋆]*University of Rome 'La Sapienza', Rome, Italy*
francesco.nasuti@uniroma1.it

Abstract

The start-up process of a liquid rocket engine is a particularly complex phenomenon, characterised by extremely challenging conditions for the system. It is therefore essential to conduct a comprehensive and accurate analysis to determine the optimal valve manoeuvring sequence that ensures a correct transition to the engine main mode with as low as possible thermo-mechanical loads on the different engine components. This is particularly pertinent when considering engines characterized by staged combustion cycles, where the presence of multiple combustion chambers in series introduces further complexities with regard to the ignition timing of each combustion chamber. This study aims to delineate the methodology for undertaking such an analysis, considering the highly complex RD-170 engine cycle, serving as a case study. Firstly, the engine cycle has been reconstructed basing on few elements available in literature (using Matlab codes and NASA CEA software), this modelling was refined iteratively and used to tune the EcosimPro model in parallel. The development of a precise representation of the engine was made possible through the implementation of a RP-1 characterisation in terms of its thermophysical and chemical properties. Secondly, in order to achieve a more precise representation of the engine while simultaneously enhancing computational efficiency, new components were introduced in the model on EcosimPro. Finally, once a reliable and accurate model of the engine had been obtained on EcosimPro environment, the study of its start-up sequence has been made possible. Several parameters influencing the RD-170 start-up transient have been analyzed (i.e. the ignition instant of the thrust chambers, the time delay of main valves openings), allowing to define a realistic start-up sequence that respects the characteristic times found in literature and, at the same time, did not expose the engine sub-systems to extreme thermo-mechanical loads. This ultimately enabled the acquisition of a set of findings and considerations that are not only beneficial for the reconstruction of the RD-170 start-up phase, but also for the analysis of future engines with cycles and characteristics analogous to those presented in this study.

1. Introduction

Throughout their operational lifespan, liquid rocket engines undergo numerous transient phases. However, the transient behavior of such engines is often less emphasized compared to their performance under steady-state conditions. While engines are typically analyzed and tested to ensure their performance meets design specifications under nominal conditions, these tests fail to account for the extreme conditions experienced during transient phases, which can lead to pressure and temperature peaks, combustion instabilities, biphasic flows or water hammer effects in the feedlines, potentially causing system failure. For this reason, it is crucial to analyze phenomena such as chill-down, start-up, throttling, and shutdown, with particular attention to the start-up transient, which is the most critical phase. While other transients like throttling and shutdown involve less significant fluctuations, the start-up process is particularly complex and stressful for the engine. Correctly analyzing this phase is essential to ensure smooth and stable achieving of the engine steady-state while preventing potential failures. Each liquid rocket engine has unique characteristics, which can vary depending on the cycle, propellant combination, and specific engine design. The start-up procedure is inherently tied to these characteristics, making it essential to thoroughly investigate the engine to ensure an efficient and functional start-up. As engines become more complex and with higher performance, the development of precise tools to analyze the start-up transient becomes even more necessary. In pump-fed engines, one of the major concerns is ensuring that turbomachinery is adequately powered before combustion ignition, especially in staged combustion engines, where proper calibration of both the main combustion

Copyright © 2025 by Samuele Corbo, Marco Galeotta, Marco De Rosa, Francesco Nasuti, Nicola Ierardo. Published by the EUCASS association with permission.

DOI: 10.13009/EUCASS2025-154

chamber and preburner ignition is crucial. The availability of software to simulate these processes can significantly reduce the need for experimental testing, thus lowering costs and development time for liquid propellant rocket engines. This paper discusses the procedure for analyzing the start-up process of a liquid rocket engine, conducted using EcosimPro software and the ESPSS libraries. The focus is on creating transient models of a rocket engine, using the RD-170 engine as a reference to observe critical phenomena associated with the complex start-up process of liquid rocket engines. The analysis of such an engine serves as an excellent example of a potential start-up sequence for future projects, particularly in this historical context where the the development of high-performance, and therefore particularly complex, liquid rocket engines is becoming increasingly widespread.

2. Methodology

In order to study the start-up transient of an engine, it is first necessary to reconstruct its steady-state functioning. If the available data are insufficient to uniquely determine the operating point of the various engine components, a preliminary procedure must be carried out to obtain this information. This is essential in order to accurately build the engine transient model. The following chapter outlines the procedure used to construct a model of the liquid rocket engine. During the preliminary analysis, MATLAB and NASA CEA software were employed to determine the operating point of the engine cycle, and to obtain nominal values for key parameters such as mass flow rate, pressure, and temperature at various engine components. Meanwhile, EcosimPro and the ESPSS libraries were utilized to construct transient models and sub-models of the engine and its components, which were subsequently used to analyze the RD-170 engine start-up process.

2.1 Engine steady-state modelling

Initially, the power balance equation for the engine shaft of the turbomachinery is considered:

$$-\sum_i \dot{m}_i^{turb}\,\Delta h_i^{turb} = \sum_i \dot{m}_i^{pump,\,ox}\,\Delta h_i^{pump,\,ox} + \sum_i \dot{m}_i^{pump,\,fuel}\,\Delta h_i^{pump,\,fuel}$$

This equation accounts for the possibility of multiple turbines or pumps operating on the same engine shaft. If there are multiple engine shafts, the procedure must be repeated for each one. Given the preliminary nature of this procedure, which will later be refined using the model developed in EcosimPro, some simplifying assumptions are made. Specifically, the ideal gas assumption is applied to the fluid processed by the turbine and the ideal liquid assumption for the fluid processes by the pumps. These assumptions lead to the following equation:

$$\sum_i \left(\dot{m}_{turb}\, C_{P_{turb}}\, T_{in}^{turb} \left(1 - \frac{T_{out}^{turb}}{T_{in}^{turb}} \right) \eta_{turb} \right)_i = \sum_i \left(\dot{m}_{ox}\, \frac{\Delta P_{ox}}{\rho_{ox}\,\eta_{ox}} \right)_i + \sum_i \left(\dot{m}_{fuel}\, \frac{\Delta P_{fuel}}{\rho_{fuel}\,\eta_{fuel}} \right)_i$$

At this point, depending on the specific cycle and the particular characteristics of the engine, this equation can be simplified in various ways. For example, in the case of staged combustion cycle engines (such as the RD-170), the mass flow rate processed by the turbine and the pumps can be related to the mixture ratio of the pre-burner (or gas generator in the case of an open cycle engine). This highlights the need to use software like NASA CEA to link the amount of propellants injected into the pre-burner (and the resulting mixture ratio) to the properties of the gas processed in the turbine, and thus to the power that can be extracted from it to drive the pumps. This procedure allows for a careful analysis of the characteristics required by the turbomachinery in terms of efficiency, once the required mass flow rates and the pressure variation of the working fluid have been determined (or vice versa). Once these preliminary values are obtained, it is crucial to ensure that the assumed values are consistent with other known or assumed characteristics of the turbomachinery, such as the angular velocity of the engine shaft, the dimensions, and the type of pump or turbine involved. In the case of the RD-170, most of this data was readily available in the literature. As a result, a detailed preliminary analysis of the turbomachinery characteristics was not necessary. This allows to reduce significantly potential sources of errors in the reconstruction of the transient model and its start-up process.

2.2 Cooling jacket modelling

The characterization of the cooling jacket plays a crucial role in the overall thermal management of the propulsion system. Moreover, during the initial transient phases, the coolant properties and its physical state are significantly influenced by the geometry and design of the cooling jacket. A precise understanding of this subsystem is essential to obtain accurate and reliable outcomes from the start-up transient analysis. For a preliminary sizing of the cooling

DOI: 10.13009/EUCASS2025-154

jacket, the first step is to model the heat fluxes generated by the hot gases within the thrust chamber. Using the NASA CEA software, a good initial approximation of the hot gas properties inside the thrust chamber, which are needed to define the heat flux profile, can be obtained. Subsequently, a nozzle profile is assumed based on the approximation of a Thrust Optimized Parabolic (TOP) nozzle using a quadratic BÃ©zier curve. The exit angle of the nozzle and the initial wall angle of the parabola are selected in accordance with the nozzle expansion ratio and length. By combining the nozzle profile and the data from the CEA software regarding the thust chamber conditions, the heat flow coefficient can be calculated using the Bartz correlation:

$$h_{Bartz} = \frac{0.026}{D_{th}} \left(\frac{C_P \mu^{0.2}}{Pr^{0.6}} \right)_c \left(\frac{P_c}{c^*} \right)^{0.8} \left(\frac{D_t}{R_{curv}} \right)^{0.1} \left(\frac{A_{th}}{A(x)} \right)^{0.9} \sigma$$

$$\sigma = \frac{1}{\left(1 + \frac{\gamma-1}{2} M^2\right)^{0.12} \left[\frac{1}{2} \frac{T_{wg}}{T_c} \left(1 + \frac{\gamma-1}{2} M^2\right) + 0.5 \right]^{0.68}}$$

where: the subscript "c" represents stagnation conditions, μ is the dynamic viscosity, C_P is the specific heat, Pr is the Prandtl number, c^* is the characteristic velocity, the subscript "th" represents throat conditions, R_{curv} is the throat radius of curvature, M is the local Mach number, T_{wg} the hot gas side wall temperature and γ is the specific heat ratio. Prandtl number and C_p are calculated considering frozen conditions.[6] This correlation gives rather accurate and reliable results only in the throat section, so modifications have been applied to it:

$$h = h_{Bartz} K_{acc} K_{inj} K_x$$

K_x is used to consider the boundary layer growth in the cylindrical part and in the nozzle since the geometric reference parameter in the original Bartz equation was the throat diameter.

$$K_x = \left(\frac{x}{x_{th}} \right)^b$$

where the coefficient "b" must be set depending on the propellant combinations.
K_{inj} instead is a correction factor used to take into account the the vaporization phenomenon near the injector plate. In the so-called combustion zone the heat flux decreases when getting closer to the injector plate. This behaviour is due to the incomplete mixing and reaction of the flow for the given injector and combustion chamber. The mixing region has a finite length where the combustion is not fully developed, therefore the heat fluxes are lower. So, this function is used in the range $x_0 \leq x \leq x_{max}$:

$$K_{inj} = \frac{1}{4} \arctan \left[7 \left(\frac{x}{x_{max}} - 0.63 \right) \right] + 0.7$$

where the combustion length x_{max} is an input value.[5]
K_{acc} is another correction factor related to the flow acceleration used to improve heat flux coefficient estimation with respect to experimental data, indeed the measured heat fluxes are lower than the calculated ones upstream and downstream the nozzle throat with the basic Bartz correlation. This behaviour is caused probably by the nozzle contour which accelerates the flow, increasing the boundary layer thickness. Instead of using the local velocity gradient to develop the correction factor, a more practicable way is to use the absolute value of the first derivative of the chamber radius with respect to the streamwise coordinate, $\left|\frac{dr}{dx}\right|$:

$$K_{acc} = \sqrt{1 - \left| \frac{dr}{dx} \right|}$$

Once this profile is obtained, the next step is the preliminary design of the cooling jacket, assuming it is not already available. This involves considering reasonable limits in terms of the minimum channel size and the thermo-mechanical loads that the walls of the thrust chamber can withstand. To model the heat exchange between the hot gases and the coolant, the following formulation is used:

$$\frac{1}{N} \frac{dQ}{dx} = h_{new} (T_{aw} - T_{coat}) d_0 = \frac{k_{coat}}{t_{coat}} (T_{coat} - T_{wg}) d_0 = \frac{k_{wall}}{t_{liner}} (T_{wg} - T_{wc}) \frac{d_1 - d_0}{ln\left(\frac{d_1}{d_0}\right)} = h_{cool} (T_{wc} - T_{cool}) d_1$$

where: N is the number of cooling channels at the axial position x, w_{ch} is the local channels width, t_{ch} is the local channels height, t_{rib} is the local channels rib thickness, t_{liner} is the local liner thickness, T_{aw} is the local adiabatic wall temperature, T_{wc} is the local coolant side wall temperature, T is the chamber temperature at the axial position x, $d_0 = w_{ch} + t_{rib} = \frac{2\pi r}{N}$ is the wall length that exchanges heat with the thrust chamber hot gases at the axial position x, $d_1 =$

DOI: 10.13009/EUCASS2025-154

$w_{ch} + 2\,t_{ch}\,c$ is the wall length that exchanges heat with the coolant at the axial position x, c is the vertical length percentage that contributes to the heat exchange with the coolant (assumed 50 %) and h_{cool} is the convective heat flux coefficient between the coolant and the wall, modelled with the Dittus-Boelter formulation.[15]
This formulation is clearly valid locally at each axial position and must be repeated for each position along the thrust chamber. The coolant temperature depends locally on the adjacent axial positions and, in particular, on the specific design of the cooling jacket. It is important to note that this procedure does not immediately yield an optimal channels geometry. Therefore, the characteristics of the cooling jacket must be updated iteratively to ensure that the subsystem is not only capable of sufficiently reducing the wall temperatures of the thrust chamber but also of avoiding excessive pressure losses experienced by the coolant as it flows through the channels.

2.3 Engine transient modelling and tuning

Once the preliminary design of the various subsystems that constitute the liquid rocket engine has been established, the subsequent step involves the development of a comprehensive engine model, which will then serve as the foundation for transient analysis. Given the inherent complexity of such engines, it is typically requisite to construct a series of sub-models representing the complete engine, with an initial focus on modelling the individual components.

2.3.1 Pump

The modelling process begins with the representation of this component, which within the EcosimPro software can be approached in two distinct ways: either directly by using the characteristic curves of the pump, when these are available, or by calculating characteristic performance parameters. These parameters are then used to reconstruct the pumps characteristic curves through interpolation, based on reference curves. The parameters involved are:

$$TDH = \frac{\Delta P}{\rho\, g}$$

$$N_s = \frac{\sqrt{Q}}{TDH^{0.75}}\,\omega$$

where: TDH is the total dynamic head, Q is the volumetric flow, N_s is the specific speed, ρ is the propellant density at pump inlet and ω is the pump angular velocity defined in rpm. These quantities can be calculated through the preliminary analysis that has been carried out, taking into account the generally known conditions of the propellants entering the pumps.

2.3.2 Turbine

In a similar manner to the pumps, the modelling of each turbine in the engine is performed. Here as well, the transient behavior of the turbine can be modeled either by directly applying characteristic curves known in advance, or by defining specific parameters used by the software to interpolate these curves from reference curves stored within the ESPSS libraries. For the turbine, these parameters are the turbine total pressure ratio and:

$$N = \frac{\omega\, r}{v_{sound}}$$

where: N is the nominal characteristic speed, ω is the angular velocity and r is the mean blade radius.
Regarding the properties of the gas entering the turbine, these must clearly be assumed according to the liquid rocket engine cycle and the preliminary analyses performed. However, this modelling procedure will be repeated iteratively to refine and enhance the accuracy of the boundary conditions. Once each transient engine model has been obtained and calibrated in EcosimPro, they will be used to update and improve the estimates made during the preliminary analysis, using the Matlab and CEA codes developed earlier. These tools will thus be employed once more to determine a new operating point for the cycle and its components under steady-state and nominal conditions, which will then serve as the new starting point for fine-tuning the models created in EcosimPro.

2.3.3 Preburner

If the engine includes a preburner (or a gas generator, similarly), as in the case of the RD-170, it must also be modeled and calibrated in EcosimPro. The characterization of the preburner represents a critical aspect of the modelling phase, as the propellant mixture ratio must be precisely controlled to ensure that the temperature, pressure, and mass flow rate of its combustion products are consistent with the power output required by the turbine under steady-state

DOI: 10.13009/EUCASS2025-154

conditions. Regarding the geometric parameters and the coefficients that govern the pressure losses across the preburner injection plate, these need to be adjusted iteratively during the preburner calibration process. These parameters indeed control both the pressure losses experienced by each propellant and their mixture ratio, therefore affecting the properties of the combustion gases exiting the preburner.

2.3.4 Thrust chamber and cooling jacket

Similarly to the preburner, the geometric parameters and the coefficients governing the pressure losses through the injection plate of the thrust chamber must be adjusted iteratively to meet both the expected pressure in the combustion chamber and the mixture ratio. Clearly, in both this case and the previous one, this tuning process must be repeated each time the boundary conditions are updated, and therefore after each iteration of the engine operating point definition. Once the thrust chamber component is tuned, it is then used to model the cooling jacket. Despite the fact that the geometries of the various channels have been defined preliminarily, the choice of the correlation used to describe the convective heat flux coefficient on the coolant side is of crucial importance, as well as the channels wall roughness. These parameters together define the actual cooling action and the pressure losses experienced by the coolant through this component.

2.3.5 Engine sub-models

Once the primary components have been modelled and tuned, the next step involves the development of progressively more complex sub-models of the engine. These sub-models enable the examination of the interdependencies between the various components, necessitating a new calibration of their respective parameters. Additionally, within these sub-models, the various pipes, valves, and secondary components, which are crucial during transient phases, are modelled and incorporated.
Through the use of these sub-models, it becomes possible to observe the effects of component coupling, which is particularly relevant for liquid rocket engines, especially those characterized by closed cycles. The results obtained from this tuning process can subsequently be utilized to refine the outcomes from the preliminary analysis, thereby enhancing the accuracy of this procedure and defining a new operating point. This updated operating point typically deviates only marginally from the previous one. This iterative process, however, allows for a more precise recalibration of the individual components, ensuring that, once the complete engine model is finalized and calibrated, it will deliver the expected nominal performance under steady-state conditions.

3. RD-170 engine

The RD-170 engine utilizes a high-performance ox-rich staged combustion cycle, operating with kerosene (RP-1) as the fuel and liquid oxygen (LOX) as the oxidizer.[8,12] It features four combustion chambers, all supplied by a single-shaft pump system, which is powered by a single-stage turbine. This turbine is driven by combustion gases from two oxidizer-rich preburners.[2,3] The propellants are pressurized through a two-stage fuel pump and a single-stage oxidizer pump, both of which are preceded by boost pumps. The fuel boost pump is powered by a hydraulic turbine, while the oxidizer boost pump is driven by a two-stage turbine. The oxidizer is entirely routed to the preburners. However, only a portion of the RP-1 is pressurized by the second stage of the fuel pump, after which it is sent to the preburners. The remaining RP-1 is directed through the cooling jackets channels of the four thrust chambers before reaching the fuel dome of the injection head. Additionally, the RD-170 features a starting system, which includes a starting tank with a diaphragm seal and a pipeline that supplies pressurizing gas. The outlet of the tank is connected to three separate lines, which link the starting system to the rest of the engine. These lines are particularly responsible for supplying triethylaluminium-filled ampoules, which are used to ignite the preburners and thrust chambers during the engine start-up process.

3.1 Start-up process

This section describes the RD-170 engine start-up process, focusing on the transient phase following engine preconditioning (purging and chill-down).[12]
At time $t = 0\ s$, the engine is in the following configuration: the fuel and oxygen have been pressurized in the propellant tanks and flow through the lines up to the shut-off valves (12, 25) and the thrust regulator valve (32). Simultaneously, the starting tank (47) is filled with kerosene. The start-up sequence begins when the starting tank (47) is pressurized, initiating the flow of fuel through the starting system lines (52, 58), which breaks the membranes of the ampoules (36, 56). At the same time, the shut-off valves (12, 25, 37) open, and the thrust regulator valve remains in its

DOI: 10.13009/EUCASS2025-154

initial position, which closes the fuel split pump (17) line (30) while allowing fuel to flow through the starting system line (52). These actions enable oxygen to fill the cavities of the two preburners (6), where it reacts with the hypergolic fuel (and also the kerosene), which is subsequently injected into the combustion chambers.

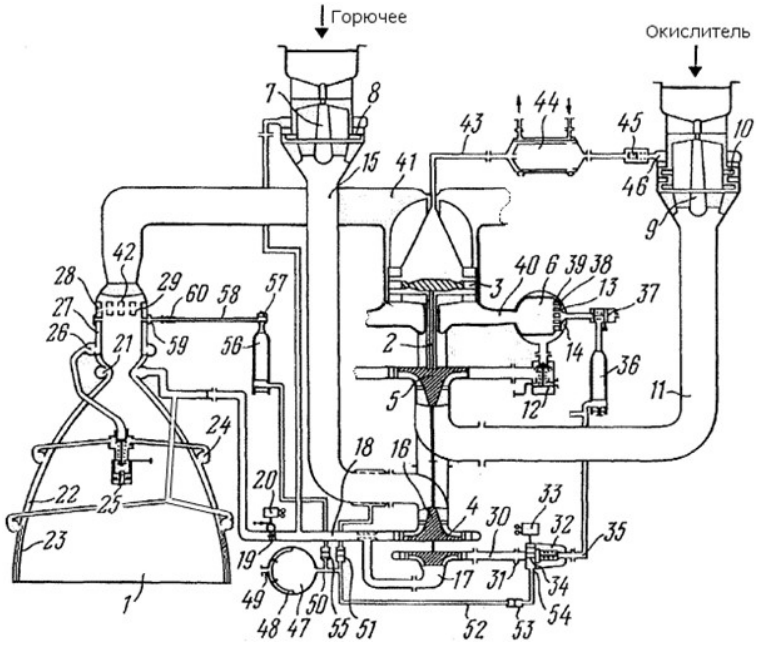


Figure 1: RD-170 pneumohydraulic diagram[9] (conventionally shown one thrust chamber and one preburner).

After the ignition of the preburners, the combustion gases flow through the turbine (3), causing the turbopump unit (2) shaft to begin rotating. These exhaust gases are then directed into the four thrust chambers (1), where they interact with the hypergolic fuel from the ampoules and the kerosene, which has filled the cooling jackets (22) and is entering the chambers. This second ignition phase is carefully timed to allow sufficient time for the turbopump unit to reach operational mode, thereby preventing back-pressure issues associated with thrust chamber ignition, which could disrupt the start-up transient. During this transient phase, the pressure downstream of the fuel pump (4) increases, which causes the starting tank check valves (53, 55) to close automatically. Concurrently, the three-way valve (32) moves to its nominal position, allowing kerosene to flow through the second stage of the fuel pump. As the system progresses toward steady-state conditions, part of the turbine exhaust gases and a portion of the kerosene downstream of the first stage of the fuel pump begin to accelerate the boost-pumps shafts, flowing through the two-stage turbine (10) and the hydraulic turbine (8), respectively. This entire procedure takes approximately 3 seconds, bringing the engine to nominal operating conditions through a smooth transient process.[12]

4. Start-up transient analysis results

Following the modelling and tuning procedure outlined previously, an accurate model of the RD-170 engine can be obtained (Figure 2). This engine model, along with its sub-models, enables the analysis of the RD-170 start-up process. The boundary conditions considered include an initial pumps inlet pressure of 3.5 bar, a pressure downstream of the chill-down line of 1 bar, and an initial start-up tank pressure of 100 bar. The inlet pressure of the pumps was selected taking into partial consideration the head increase provided by the boost pumps. In particular, the inlet pressure was increased from 3.5 bar to 10 bar after the opening of the lines through which the propellants are supplied to the turbines driving the boost pumps. Although the model created is sufficiently accurate and effectively simulates the main subsystems of the actual liquid rocket engine, there are two notable differences: first, neither the boost pumps nor their respective turbines are included; second, the presence of hypergolic fluid in the components simulating the ampoules has not been considered. The first assumption is linked to the lack of sufficient information to enable the modelling of complex components such as pumps and turbines, and to avoid introducing additional sources of uncertainty into the model. Conversely, the utilization of hypergolic fluid for the purpose of facilitating combustion chambers ignition has been partially incorporated into the model by considering relatively wide mixture ratio ignition limits. This approach eliminates the need to introduce an additional propellant into the simulation, which would otherwise have required extensive characterization, as is the case with RP-1, and it would also have considerably

DOI: 10.13009/EUCASS2025-154

increased the computational cost of the simulations. Finally, to ensure the system reaches a steady and stable condition before the start-up process begins, the engine valve opening sequence was defined to start at time 0.5 seconds, which corresponds to the opening of the main oxygen valves.

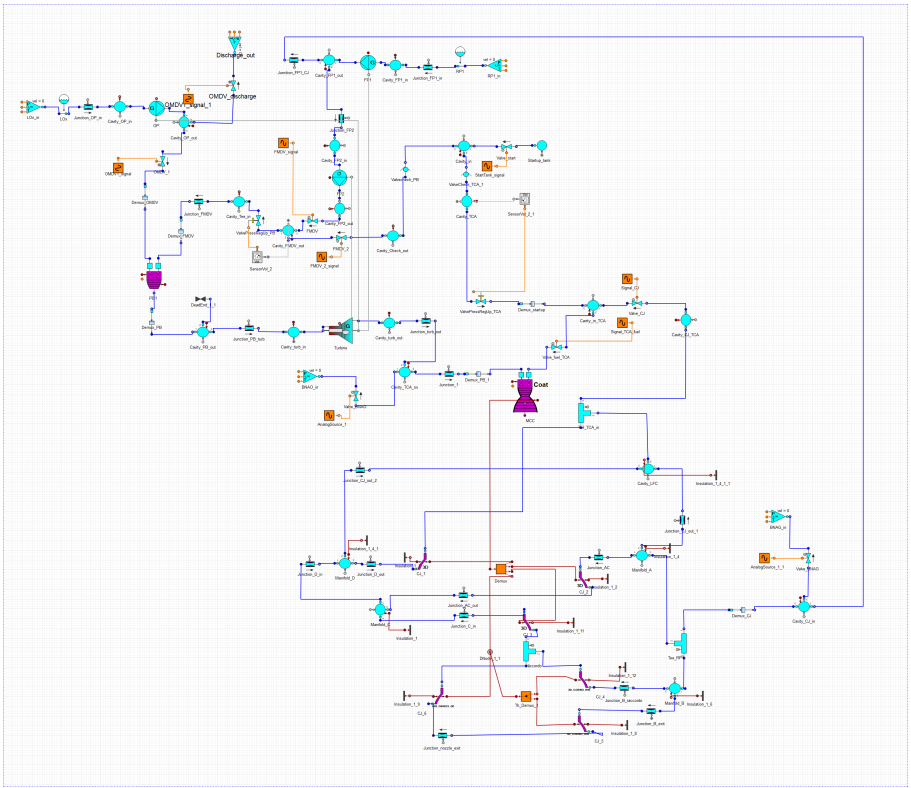


Figure 2: Engine schematic.

4.1 RP-1 characterization

Before starting with the engine analysis, a precise characterization of the fuel is needed, indeed an accurate knowledge of thermophysical properties is a prerequisite to a model development of an engine using kerosene rocket propellant (RP-1).[10] Unlike oxygen or other rocket propellants as methane and hydrogen, RP-1 indeed is a complex mixture of several hundred components, thus to obtain reliable results it is necessary to define the fuel chosen as reference and to define properly how its properties vary with pressure and temperature.[13] Moreover the ESPSS library version available[4] is not provided with RP-1 as fuel, so it is necessary to characterize this fuel in order to perform the start-up transient analysis of the engine.
At EcosimPro level, RP-1 has been defined as a perfect liquid, thus a new data file ($PfLiqUsr4.dat$) has been added in the PROP_TABLES folder inside the FLUID_PROPERTIES library, defining the following properties as a function of the temperature: density, specific heat at constant pressure, thermal conductivity, speed of sound and viscosity. These RP-1 features have been selected comparing different studies, where it was experimentally tested to measure its behaviour under several conditions (in terms of pressure and temperature).[1,10,13]
Furthermore, kerosene must be described also from a chemical point of view. This fuel indeed is a mixture of several hydrocarbons and defining a single chemical formula is very complex. In particular, an accurate RP-1 chemical composition and its related heat of formation are necessary to obtain reliable results when combustion takes place, especially when exhaust gases coming from a preburner are used to drive the turbine, as in the RD-170. Therefore $C_{12}H_{24}$ has been chosen as one-formula surrogate fuel formulation with an enthalpy of formation equal to -92.200 $\frac{kcal}{mol}$, that was validated exactly on the RD-170 engine performance.[14] This modelling has been implemented in the ESPSS library, modifying the *thermo.lib* file present in the PROP_TABLES. In particular, first of all the *thermo.inp* file was modified, adding the new RP-1 parameters,[14] and then exploiting NASA CEA software, the new *thermo.lib* file has been created from its input file.[11] Through this procedure an accurate enough RP-1 characterization has been added to the ESPSS library, giving the possibility to devise reliable rocket engine simulations when this fuel is used.

DOI: 10.13009/EUCASS2025-154

4.2 New EcosimPro components

To achieve a more accurate representation of the RD-170 engine in EcosimPro, new components were specifically developed to enhance the modelling of the engine start-up process. These components were designed to address the complexities involved in simulating various subsystems and their interactions during the engine transient phases.

4.2.1 Thermal demultiplexer

A key component introduced for this purpose is the thermal demultiplexer, which connects the different sections of the thrust chamber to several cooling jacket branches. The standard cooling jacket component does not support a variable number of channels along the axial coordinate, nor does it allow for different wall materials. The thermal demultiplexer splits a single thermal port into four separate thermal ports, providing greater flexibility. This component is divided into "$n_1 + n_2 + n_3 + n_4$" nodes, where each "n_i" represents the number of nodes for a given section. Each node ensures continuity in temperature and heat flux between the two components connected to the thermal demultiplexer.

4.2.2 New cooling jacket

This component is inherited from the cooling jacket already implemented in the COMB_CHAMBER library.[4] However this new element allows to fix the rib thickness of the channels along the axial direction. In particular, previously it was computed from the other user-defined data as:

$$t_{rib} = 0.5 \left(\frac{\pi D}{N_{channel}} - w_{channel} \right)$$

Instead, with the new cooling jacket it is possible to define a 1D non-dimensional table ("*trib_vs_L*") which defines the rib thickness with respect to the axial coordinate. This degree of freedom has been added in order to properly model parallel sequential cooling jackets (1-$\frac{1}{2}$ cooling channels), otherwise a much bigger inter-channel wall thickness would result.

4.2.3 Fluid demultiplexer

The fluid demultiplexer component was developed to optimize simulation efficiency by reducing computational time. The RD-170 engine, indeed, exhibits notable symmetries, including two identical preburners and four equal thrust chambers. Consequently, the component is designed to maintain the same intensive variables, while scaling the extensive variables by a user-defined factor, α.

4.3 Thrust chambers ignition time effect

The ignition timing of the thrust chambers plays a central role when studying such a process. It is crucial that this phenomenon does not occur too prematurely, as it could lead to a sudden halt of the turbomachinery, resulting in a failure of the start-up procedure. Conversely, if the ignition is delayed for too long, excessive mechanical loads may be placed on the various components of the engine, as will be discussed. Specifically, the timing of the opening of the "Valve_CJ" and "Valve_fuel_TCA" valves (Figure 2) is of paramount importance, as the system is highly sensitive to this moment. These valves regulate the ignition of the thrust chambers. It has been observed (Figure 3) that, opening the valve controlling the flow of RP-1 into the thrust chambers just one second after the OMDV valve is opened, leads to a significant deceleration of the turbomachinery, effectively halting the start-up process. However, a successful initial transient can be achieved when this opening is delayed by 100 ms (Figure 4). Therefore, the modified sequence (Table 1) allows the engine to start, even though ignition of the thrust chambers results in a considerable deceleration of the pumps. Consequently, it is of interest to observe not only how the engine transitions from a failed transient to a successful one only by shifting this instant by 0.1 seconds, but also the effects of further delaying the opening of these valves on the transient. A parametric analysis of the value t_{CJ} (and t_{TCA}, which is equal to it) is therefore carried out, with a 100 ms delay applied in each case, resulting in the consideration of four distinct simulations with four varying opening times for the "Valve_CJ" and the "Valve_fuel_TCA" ($t_{OMDV} + 1.1\ s$, $t_{OMDV} + 1.2\ s$, $t_{OMDV} + 1.3\ s$, $t_{OMDV} + 1.4\ s$). It is evident that the activation of the thrust chambers at a later point in time results in a notable increase in the pressure within the system (Figure 5).

DOI: 10.13009/EUCASS2025-154

Event	Parameter	Time [s]
OMDVs are opened	t_{OMDV}	0.500
Start-up tank is opened	$t_{start} = t_{OMDV} + 15\,ms$	0.515
FMDV_2 is opened	$t_{FMDV} = t_{OMDV} + 15\,ms$	0.515
FMDV_2 is closed	$t_{FMDV_2} = t_{OMDV} + 70\,ms$	0.570
FMDV is opened	$t_{FMDV_2} = t_{OMDV} + 70\,ms$	0.570
Valve_CJ is opened	$t_{CJ} = t_{OMDV} + 1.100\,s$	1.600
Valve_fuel_TCA is opened	$t_{TCA} = t_{OMDV} + 1.100\,s$	1.600
Valve_BNAO is opened	$t_{BNAO} = t_{CJ} + 0.500\,s$	2.100
Valve_BNAG is opened	$t_{BNAG} = t_{CJ} + 0.500\,s$	2.100

Table 1: Engine model valve opening sequence.

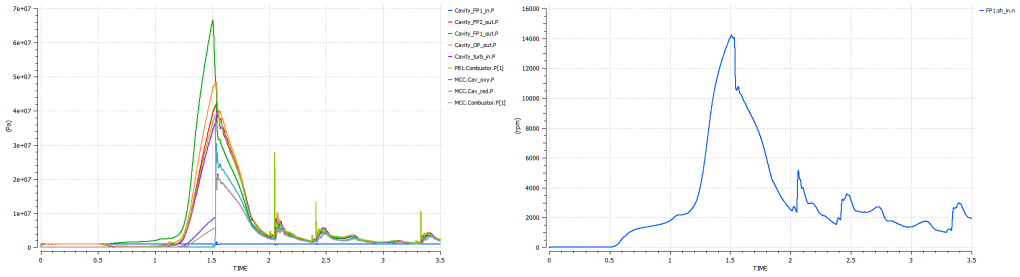


Figure 3: Engine start-up results ($t_{CJ} = t_{OMDV} + 1.0\,s$). Static pressures and turbomachinery shaft angular velocity during the transient.

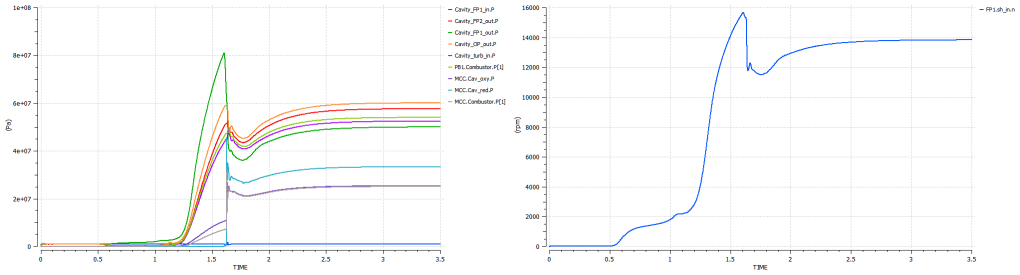


Figure 4: Engine start-up results ($t_{CJ} = t_{OMDV} + 1.1\,s$). Static pressures and turbomachinery shaft angular velocity during the transient.

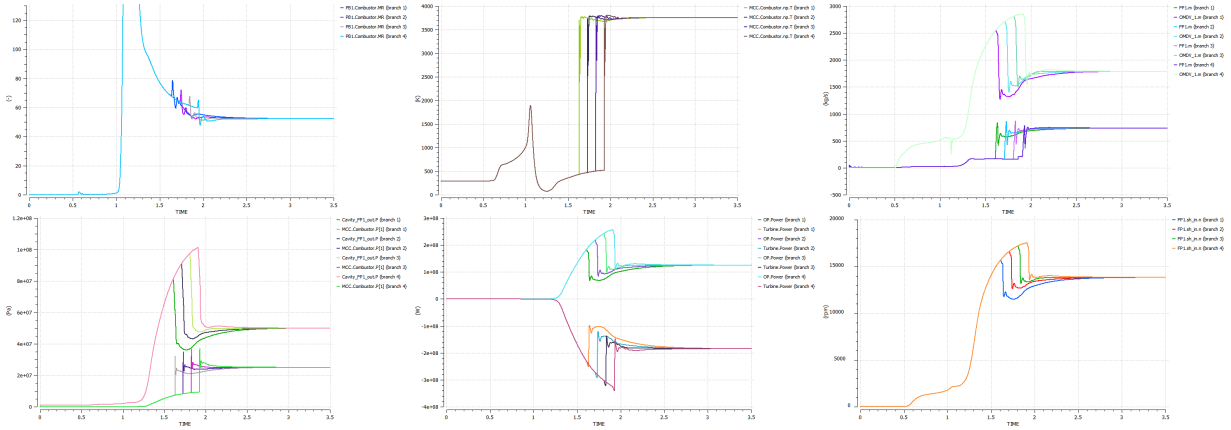


Figure 5: Engine start-up results (varying t_{CJ}). Preburner mixture ratio, combustion chamber temperature, mass flow rates, static pressures, turbomachinery shaft power and angular velocity during the transient.

DOI: 10.13009/EUCASS2025-154

This phenomenon can be observed in the pressure downstream of the fuel pump first stage (FP1), which, represents the highest pressure value in the system. Therefore, a delay in the ignition of the thrust chambers results in the system being subjected to elevated mechanical loads. Conversely, it can be observed that the delayed opening of the "Valve_CJ" results in a reduction in the amplitude of the oscillations exhibited by the engine variables. In particular, the undershooting (particularly evident when observing the angular velocity of the turbomachinery) tends to disappear if t_{CJ} is increased. It is noteworthy that the point of operation of the pumps undergoes a change upon the triggering of the thrust chambers, as evidenced by the concomitant increase in temperature and pressure within the combustion chambers. Indeed, it is evident that the power (with the turbine and the oxygen pump, OP, serving as illustrative examples, although a similar trend is observed in the other cases) undergoes an immediate decline following the ignition of combustion within the thrust chambers. This reduction in power results in a decrease in the heads supplied by the various pumps, but it has two opposite effects on the mass flow rates processed by the different pumps. Indeed, while the oxygen flow rate declines significantly, the RP-1 mass flow rate processed by fuel pump first stage increases markedly. This is attributable to the fact that the operating point of the pumps varies as a consequence of the opening of the "Valve_CJ" and the "Valve_fuel_TCA". The rise in flow rate through FP1 is understandable when one considers that by opening these valves, fuel is permitted to flow through the cooling jacket and not only towards the preburners. It can thus be concluded that the engine is subjected to excessively high pressures if the "Valve_CJ" is opened too late. This is an unfavourable situation that should be avoided. Therefore, the choice of an optimal value for chamber ignition is fundamental in order to first of all have a successful engine start-up, but at the same time not to subject the various subsystems to extremely stressful conditions.

4.4 Pumps behaviour during the start-up transient

It is of particular interest to observe the operation of the pumps during their initial stages. The initial acceleration of the turbopump, in particular, can be attributed to the fact that the inlet oxygen pressure is rather higher than the ambient pressure. During the initial phases, indeed, no working fluid is present within the turbine, thus rendering it unable to drive the pumps. This results in a tank-head oxygen pump initial acceleration, but concurrently, the fluid flowing through it experiences a decrease in pressure. Specifically, this pump undergoes an autonomous rotation as a consequence of the impingement of high-pressure propellant on its blades.
This apparently anomalous pump behaviour can be elucidated through an examination of the pump behaviour in the Karman-Knapp diagram (Figure 6).

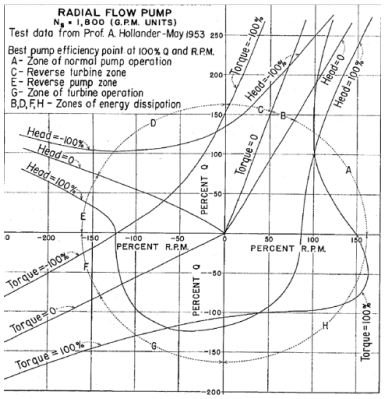


Figure 6: Karman-Knapp circle diagram.[7]

It is evident that there are a multitude of operational regimes for pumps, which are contingent upon the values of various parameters, such as torque, head, volumetric flow rate, and angular velocity. In this study, particular attention is paid to three regimes that characterize the RD-170 pumps during the start-up transient, wherein both the flow rate and angular velocity are positive. The initial operating regime is designated the "reverse turbine zone" (zone C in Figure 6). Where despite the pump is operating with a negative head, it is capable of providing power and, consequently, torque. Proceeding in a clockwise direction, we arrive at the operating regime defined as the "energy dissipation zone" (zone B in Figure 6). The latter is characterized by a negative head and a positive percentage torque, indicating that the pump is receiving power. Finally, the final zone of the pump functioning that will be discussed is that of normal operation (zone A in Figure 6). This is the region where the pump is receiving power, i.e. conventionally negative, but positive in percentage terms, and at the same time has a positive head. This implies that there is an increase in fluid pressure as it passes through the pump. Therefore, by observing each pump behaviour

DOI: 10.13009/EUCASS2025-154

during the RD-170 start-up process in comparison with that of the torque and head isocurves and contrasting it with the known behaviour of a purely centrifugal pump,[7] it is possible to discern the various operating regimes of the pump with clarity.
So, first of all, it is possible to notice that (Figure 7), upon opening the OMDV valve (at 0.5 s), an initial phase begins wherein the oxygen pump (OP) generates power (and thus torque), yet concurrently, the pressure of the fluid traversing it decreases (i.e., negative head). Similarly, this behaviour can be observed, albeit less clearly, in the split pump of RP-1 (FP2), while in the first stage of the fuel pump (FP1), none of this can be seen. Moreover, the angular velocity of the pumps trend (Figure 7) allows for the observation of the speed values at which these phases occur. In particular, the red lines represent the changes in operating mode of the OP, while the black lines represent those of the FP2. Furthermore, the dotted line indicates the point at which the pump stops supplying torque, while the dash-dot line indicates the change from negative to positive pump head. In order to gain insight into the operational characteristics of the pumps under examination, it is now appropriate to analyze the trends displayed on the respective Karman-Knapp diagrams. This will facilitate the identification of the different zones of operation experienced by each pump. Prior to undertaking this analysis, it is first necessary to define the curves that describe the operational characteristics of the various pumps. As previously stated, the curves describing the behaviour of the pumps during the transient are obtained from EcosimPro by interpolation or extrapolation from those already implemented within it, as a function of the specific speed N_s.

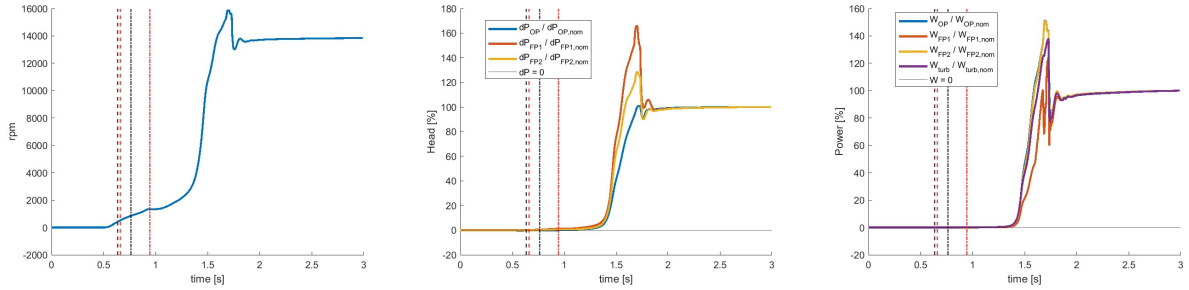


Figure 7: Pumps angular velocity, percentage head and percentage power values during the engine start-up transient.

In particular, within EcosimPro there are three different reference curves in the planes (θ,wh) and (θ,wt), which are defined for three different types of standard pumps characterised by three different values of specific speed: 25 $\frac{m^{\frac{3}{4}}}{\sqrt{s}}$ rpm (radial flow pump), 147 $\frac{m^{\frac{3}{4}}}{\sqrt{s}}$ rpm (mixed flow pump), 261 $\frac{m^{\frac{3}{4}}}{\sqrt{s}}$ rpm (axial flow pump).

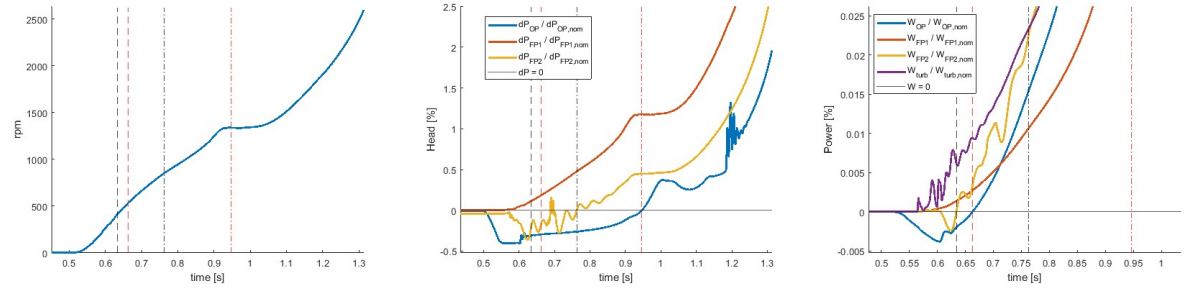


Figure 8: Pumps angular velocity, percentage head and percentage power values during the engine start-up transient (zoom immediately after the OMDV opening).

Subsequently, considering the respective N_s for each engine pump the characteristic curves in the planes (θ,wh) and (θ,wt) are obtained by interpolation or extrapolation, depending on the specific N_s, from the three reference curves (Figure 9). Once the trends of wh and wt are defined as functions of θ, it is possible to obtain the isocurves of head and torque on the Karman-Knapp diagram for the RD-170 pump system. Specifically, after dividing the domain of θ into four regions (Figure 9), the values of volumetric flow rate and angular velocity, normalized with respect to their nominal values, are calculated for each θ (and the corresponding wt and wh):

$$n_i = \frac{Q_i}{Q_R} = \pm \frac{\frac{T}{T_R}}{wt_i\,[1 + \tan^2(\theta_i - \pi)]}$$

DOI: 10.13009/EUCASS2025-154

$$v_i = \frac{\omega_i}{\omega_R} = \pm\, n_i\, \tan(\theta_i - \pi)$$

where the signs are chosen based on the specific θ range (Figure 9). Four different values are considered for the percentage of head and torque:-10%, 0%, 50%, 100%.

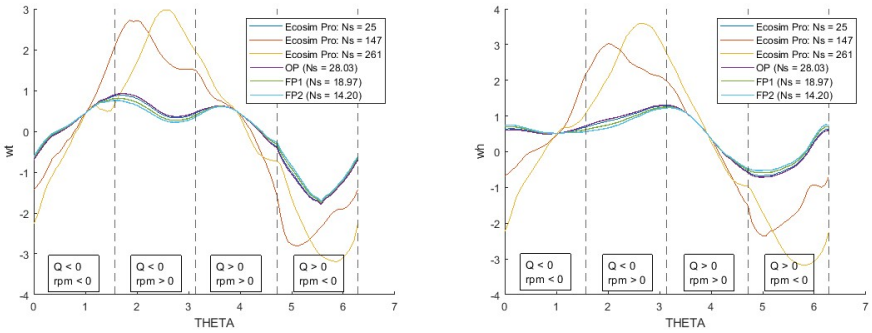


Figure 9: Dimensionless torque (wt) and head (wh) with respect to θ trends in the extended domain of the engine pumps and EcosimPro reference pumps.

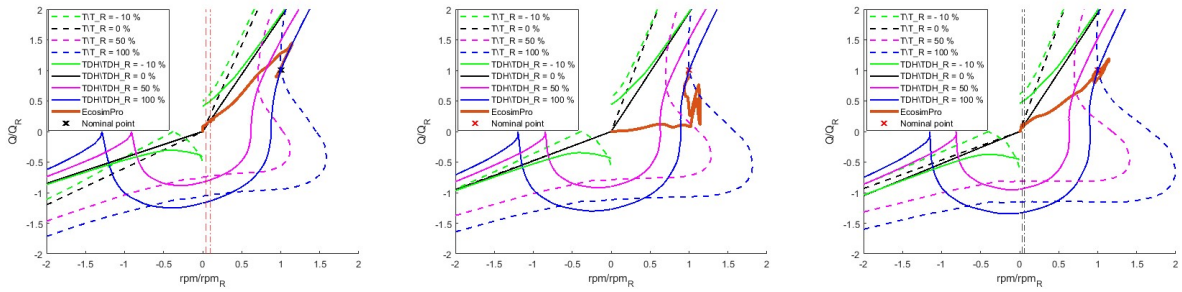


Figure 10: Oxygen, RP-1 first and second stages pumps during the engine start-up transient on the Karman-Knapp diagram with torque and head isocurves.

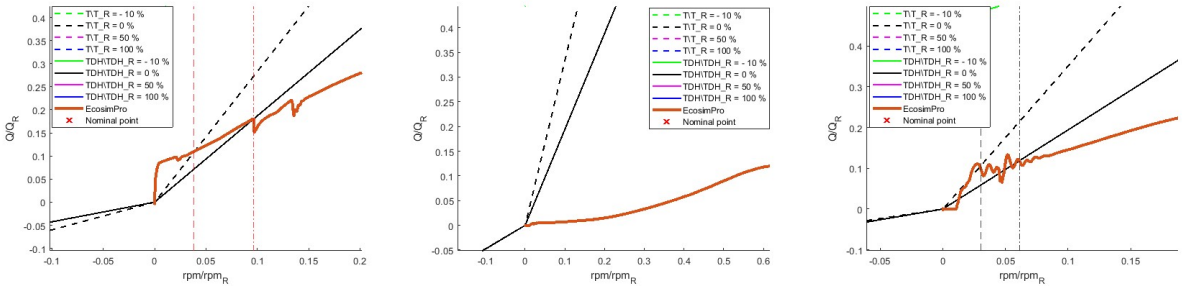


Figure 11: Oxygen, RP-1 first and second stages pumps during the engine start-up transient on the Karman-Knapp diagram with torque and head isocurves (zoom immediately after the OMDV opening).

This procedure results in the acquisition of all the isocurves for head and torque for each pump within the Karman-Knapp diagram (Figure 10). Consequently, the set of points traversed during the transient is plotted for each pump in terms of volumetric flow rate versus angular velocity, both in percentage values relative to nominal steady-state conditions, together with the aforementioned isocurves. This procedure allows the various operational regimes of a pump to be obtained, as well as providing information on the extent to which acceleration occurs in each of these regimes. It is therefore of interest to observe that both the oxygen pump and the second stage of the fuel pump traverse all three of the aforementioned pump operating zones. It is evident that as soon as the OMDV is opened and the pumps start to accelerate (Figure 8), the flow rate through the oxygen pump rises rapidly, resulting in this

DOI: 10.13009/EUCASS2025-154

pump entering the reverse turbine mode (Figure 11). As previously stated, this initiates the supply of power, yet concurrently, the oxygen flow through the pump reduces its pressure. In contrast, FP1 absorbs power and provides head immediately, entering normal operation. Finally, the FP2 exhibits a peculiar behaviour. Initially, it receives the power supplied by the OP and enters the "normal" operating regime. However, it then immediately accelerates, increasing the flow rate processed by this pump. This causes the pump to transition from one operating regime to another, first that of energy dissipation and then that of reverse turbine. These trends are also evident when observing the pressure and power trends of the pumps. Subsequently, the turbine initiates the processing of flow, thereby supplying power to the pumps. This enables the pumps to accelerate, resulting in the transition of all three pumps into a normal operating regime. The angular speed values and times at which the pumps switch from one operating regime to another are presented in Table 2.

Oxygen Pump				
Operating regime	ω_{in} [rpm]	ω_{fin} [rpm]	t_{in} [s]	t_{fin} [s]
Reverse Turbine	0	534.5	0	0.663
Energy dissipation	534.5	1338.45	0.663	0.946
Normal pump	1338.45	13850	0.946	3
Fuel Pump first stage				
Operating regime	ω_{in} [rpm]	ω_{fin} [rpm]	t_{in} [s]	t_{fin} [s]
Normal pump	0	13850	0	3
Fuel Pump second stage				
Operating regime	ω_{in} [rpm]	ω_{fin} [rpm]	t_{in} [s]	t_{fin} [s]
Reverse Turbine	0	413.3	0	0.634
Energy dissipation	413.3	833.7	0.634	0.756
Normal pump	833.7	13850	0.756	3

Table 2: Pumps angular velocities and times defining the various functioning regimes.

4.5 Final valves sequence

Ultimately, following the completion of the parametric analyses and the evaluation of the influence of various parameters on the start-up transient of the RD-170 engine, a final valve opening sequence was selected, taking into account the results obtained (Table 3).

Event	Parameter	Time [s]
OMDVs are opened	t_{OMDV}	0.500
Start-up tank is opened	$t_{start} = t_{OMDV} + 15\,ms$	0.515
FMDV_2 is opened	$t_{FMDV} = t_{OMDV} + 15\,ms$	0.515
FMDV_2 is closed	$t_{FMDV_2} = t_{OMDV} + 70\,ms$	0.570
FMDV is opened	$t_{FMDV_2} = t_{OMDV} + 70\,ms$	0.570
Valve_CJ is opened	$t_{CJ} = t_{OMDV} + 1.050\,s$	1.550
Valve_fuel_TCA is opened	$t_{TCA} = t_{OMDV} + 1.100\,s$	1.600
Valve_BNAO is opened	$t_{BNAO} = t_{CJ} + 0.500\,s$	2.050
Valve_BNAG is opened	$t_{BNAG} = t_{CJ} + 0.500\,s$	2.050

Table 3: Engine model final valve opening sequence.

Specifically, the opening of the valves regulating the fuel mass flow through the cooling jackets and into the thrust chambers was slightly anticipated. This adjustment was made to reduce the peak angular velocity of the pumps while ensuring that ignition of the thrust chambers does not occur prematurely, thereby avoiding engine start-up failure. The results (Figure 12) show that the transient phase lasts approximately three seconds. This is consistent with values reported in the literature,[12] confirming that the selected cavity volumes and turbomachinery mechanical inertias are in good agreement with those of the actual engine. However, the engine behavior during the transient still presents certain features that lead to a less smooth start-up sequence, with the engine experiencing mechanical loads higher than would be optimal. A prominent example is the pressure peak observed downstream of the first stage of the RP-1 pump (FP1), which, despite the reduction achieved through the application of the parametric analysis results, remains present and indicates that further optimization is required. This spike is primarily due to the fact that, as long as the valve upstream of the cooling jacket remains closed, the fuel flow through FP1 is equal to that through the split pump

DOI: 10.13009/EUCASS2025-154

(FP2). As a result, the head supplied by FP1 is significantly higher than it should be. It is of particular importance to note that the ignition of the thrust chambers is contingent upon the pumps reaching a very high angular velocity, which is almost equal to the nominal pumps speed. This causes the undesired pressure peak downstream of FP1. This start-up transient feature is related to the valve opening sequence. As previously stated, this is associated with the selection of t_{CJ} and, consequently, the determination of the point in time at which the thrust chambers are ignited. One potential approach to improve the obtained start-up transient could be to consider partial opening positions for the main valves (OMDV and FMDV). Therefore, one potential solution is to reduce the opening section of the valves during the transient period preceding the thrust chambers priming. This would decrease the flow rate through the turbine, reducing the acceleration of the pumps and the pressure peak. Additionally, igniting the thrust chambers with a lower flow rate would prevent the failure of the starting process caused by turning on the thrust chambers before the pumps reach a sufficient angular velocity.
It is also noteworthy that the transient exhibits two distinct temperature peaks in the preburners between 0.5 and 1 seconds, which occur immediately after ignition. This phenomenon shall be avoided to prevent thermal overstressing of the engine, particularly the turbine situated downstream of the preburners. The temperature trend observed within the preburners can be attributed to two key factors: the quantity of RP-1 injected from the engine secondary starting system and the rapidity with which the oxygen and RP-1 mass flow rates processed by the pumps increase. These factors exert a significant influence on the mixture ratio within the two preburners. This phenomenon could also be rectified by regulating the OMDV and FMDV cross section. Indeed, by accurately calibrating the quantity of propellants fed into the preburners, it is possible to modify the mixture ratio and maintain it more constant during the start-up transient.

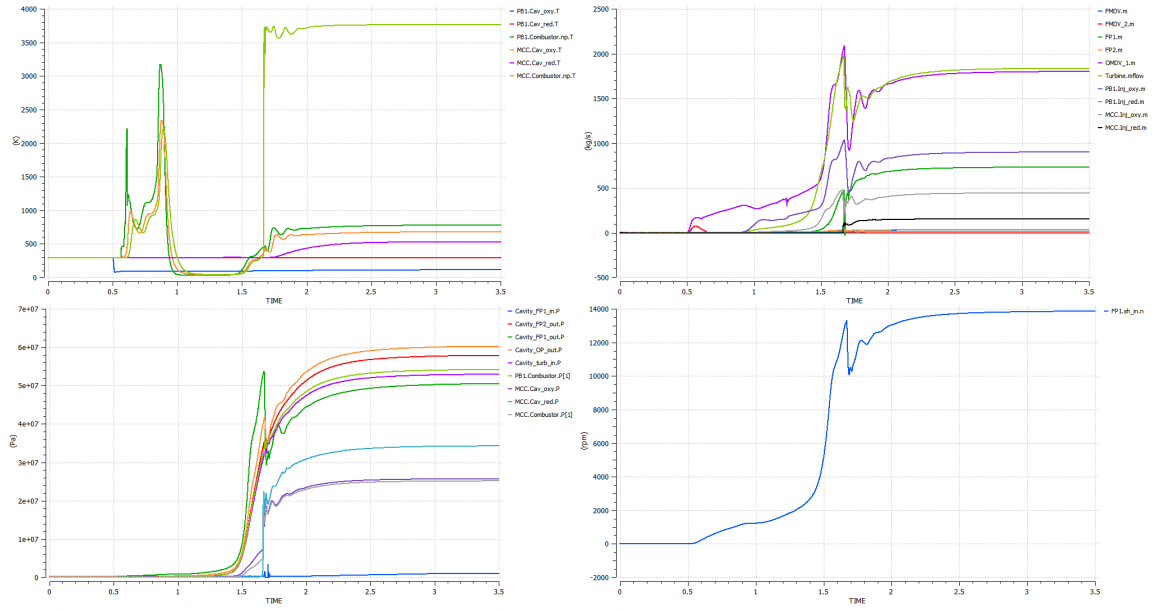


Figure 12: Engine start-up transient final results.

It can thus be stated that the issues delineated in this paragraph may be addressed by contemplating partial opening positions for the main valves (OMDV and FMDV). In the absence of detailed information regarding this specific valves characteristic and the considerable computational cost that would be incurred by conducting a sufficiently detailed parametric analysis of the various valves features, including flow regulation modes, opening and closing characteristic times, these additional modifications have not been incorporated into the subsequent work. The implementation of these elements, in addition to a more precise modelling of the preburners and boost pump lines, would certainly enhance the accuracy of the results, bringing them closer to those of the actual engine.

5. Conclusions

It has been shown that, by following the proposed methodology, it is possible to accurately reconstruct the start-up process of a highly complex engine such as the RD-170, using only the data available in the literature. The analyses carried out on this engine have highlighted how the start-up transient is characterized by a multitude of complex phenomena arising from the dynamic coupling between various components. These interactions are critical and

DOI: 10.13009/EUCASS2025-154

require detailed investigation to avoid engine failure. Moreover, the development of accurate yet computationally efficient models has enabled an in-depth analysis of the critical events occurring during this transient phase. This approach allowed the reproduction of a realistic start-up sequence, consistent with data reported in the literature. This was made possible, also through the definition of a valve opening sequence aimed at minimizing the thermo-mechanical loads experienced by the different engine components during start-up. Further improvements could be pursued in future work to enhance the accuracy of the results. In particular, a more refined representation of the boost pumps lines and preburners, along with the implementation of partial opening positions for the main valves, would contribute to a more precise simulation of the transient behaviour. Nevertheless, the model developed in this work, along with the newly created components and the analyses performed, represents a solid reference framework for conducting transient analyses on complex liquid rocket engines, especially those featuring combustion chambers arranged in series or in parallel.
This methodology could serve as a useful tool for future studies focused on the design, validation, and optimization of next-generation propulsion systems, where transient behaviour plays an increasingly crucial role.

References

[1] IM Abdulagatov and ND Azizov. Heat capacity of rocket propellant (RP-1 fuel) at high temperatures and high pressures. *Fuel*, 90(2):563–567, 2011.

[2] Alexei Pogosovich Adzhian, Vladimir Jurievich Bogushev, Valentina Dmitrievna Kolesnikova, Alexandr Mikhailovich Samsonov, Jury Anatolievich Tjurin, and Boris Ivanovich Katorgin. *Gas generator for liquid propellant rockets*. US Patent 6244040 B1, June 12, 2001.

[3] Alexei Pogosovich Adzhian, Vladimir Jurievich Bogushev, Alexandr Mikhailovich Samsonov, and Jury Anatolievich Tjurin. *Gas generator module*. US Patent 6212878 B1, April 10, 2001.

[4] Empresarios Agrupados. 2019. ESPSS EcosimPro Libraries User Manual Version: 3.3.0.

[5] Astrium and TU Dresden. Final report on data correlation and evaluation of test results phase 1 part 1. *Internal ESA contractor report GSTP-2-TN-06-Astrium, Astrium*, 2001.

[6] DR Bartz. Turbulent boundary-layer heat transfer from rapidly accelerating flow of rocket combustion gases and of heated air. *Advances in Heat Transfer*, 2:1–108, 1965.

[7] Benjamin Donsky. Complete pump characteristics and the effects of specific speeds on hydraulic transients. *Journal of basic engineering*, (83):685–699, 1961.

[8] Boris Katorgin, Feliks Chelkis, and Charles Limerick. The RD-170, a different approach to launch vehicle propulsion. *29th Joint Propulsion Conference and Exhibit*, page 2415, 1993.

[9] Boris Ivanovich Katorgin, Vladimir Konstantinovich Chvanov, Gennady Grigorievich Derkach, Jury Vasilievich Movchan, Felix Jurievich Chelkis, Vadim Iliich Semenov, and Leonid Alexeevich Tolstikov. *Liquid-propellant rocket engine with turbine gas afterburning*. US Patent 6226980 B1, May 8, 2001.

[10] Joe W Magee, Thomas J Bruno, Daniel G Friend, Marcia L Huber, Arno D Laesecke, Eric Lemmon, Mark O McLinden, Richard A Perkins, Jason A Widegren, et al. Thermophysical properties measurements and models for rocket propellant RP-1: Phase I. 2007.

[11] Bonnie J McBride. *Computer program for calculation of complex chemical equilibrium compositions and applications*, volume 2. NASA RP-1311, NASA Lewis Research Center, 1996.

[12] Cosmonautics News. http://lpre.de/.

[13] Stephanie L Outcalt, Arno Laesecke, and Karin J Brumback. Thermophysical properties measurements of rocket propellants RP-1 and RP-2. *Journal of Propulsion and Power*, 25(5):1032–1040, 2009.

[14] Ten-See Wang. Thermophysics characterization of kerosene combustion. *Journal of Thermophysics and Heat Transfer*, 15(2):140–147, 2001.

[15] H Ziebland and RC Parkinson. *Heat transfer in rocket engines*, volume 148. North Atlantic Treaty Organization, Advisory Group for Aerospace Research, 1971.